ACS NANO
Cite This: ACS Nano 2019, 13, 5939–5946
www.acsnano.org

ARTICLE

# Understanding Enantioselective Interactions by Pulling Apart Molecular Rotor Complexes

Amanda M. Larson,[†] Kyle Groden,[‡] Ryan T. Hannagan,[†] Jean-Sabin McEwen,*[,‡,¶,§,∥,⊥] and E. Charles H. Sykes*[,†]

[†]Department of Chemistry, Tufts University, Medford, Massachusetts 02155, United States
[‡]The Gene and Linda Voiland School of Chemical Engineering and Bioengineering, Washington State University, Pullman, Washington 99164, United States
[¶]Department of Chemistry, Washington State University, Pullman, Washington 99164, United States
[§]Department of Physics, Washington State University, Pullman, Washington 99164, United States
[∥]Department of Biological Systems Engineering, Washington State University, Pullman, Washington 99164, United States
[⊥]Institute of Integrated Catalysis, Pacific Northwest National Laboratory, Richland, Washington 99352, United States

Supporting Information

**ABSTRACT:** **Enantioselective interactions underpin many important phenomena from biological mechanisms to chemical catalysis. In this regard, there is great interest in understanding these effects at the molecular level. Surfaces provide a platform for these studies and aid in the long-term goal of designing heterogeneous enantiospecific interfaces. Herein we report a model system consisting of molecular rotors, one intrinsically chiral (propylene oxide) and one that becomes chiral when adsorbed on a surface (propene). Scanning tunneling microscopy (STM) measurements enable the chirality of each individual molecule to be directly visualized, and density functional theory based calculations are performed to rationalize the chiral time-averaged appearance of the molecular rotors. While there are no attractive intermolecular interactions between the molecular species themselves, when mixed together there is a strong preference for the formation of 1:1 heteromolecular pairs. We demonstrate that STM tip-induced molecular manipulations can be used to assemble these complexes, examine the chirality of each species, and thereby interrogate if their interactions are enantioselective. A statistical analysis of this data reveals that intrinsically chiral propylene oxide preferentially binds one of the enantiomers of propene with a 3:2 ratio, thereby demonstrating that the surface chirality of small nonchiral molecules can be directed with a chiral modifier. As such, this investigation sheds light onto previously reported ensemble studies in which chirally seeded layers of molecules that are achiral in the gas phase can lead to an amplification of enantioselective adsorption.**

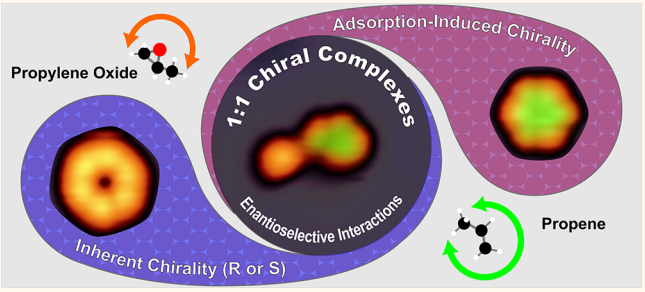


**KEYWORDS:** *enantioselectivity, single-molecule, STM, Cu(111), diastereomers, chiral modifier*

Chirality is manifested at the molecular level as two mirror-image versions of a given molecule called enantiomers. These enantiomers behave differently when interacting with other chiral species. In chemistry, enantioselectivity occurs when one enantiomer of a chiral product is formed in favor of another, thereby breaking the inherent symmetry of the system. Often subtle and difficult-to-control catalytically, enantioselectivity can differentiate the reaction pathways toward the desired enantiomer, which is of importance to pharmaceuticals production.[1] Industry heavily relies on homogeneous catalysts or separations for enantioselective chemistries, but heterogeneous catalysis offers enticing advantages for further development as chiral catalysts. To this end, a handful of reactions have exhibited enantioselectivity when the heterogeneous catalyst is modified with chiral molecules.[2−17] Given the complexity of heterogeneous reaction mechanisms and the additional enantioselective considerations, understanding these important phenomena is incredibly challenging.

Enantioselective heterogeneous catalysis originates in the enantiospecific interactions between nonchiral reactants and chiral catalytic active sites. There are three commonly discussed types of enantioselective mechanisms: (i) 1:1 interactions between the reactant and chiral modifier; (ii)

Received: March 5, 2019
Accepted: May 9, 2019
Published: May 9, 2019






DOI: 10.1021/acsnano.9b01781
ACS Nano 2019, 13, 5939–5946

surface templating by the modifier that renders the exposed surface chiral; and (iii) inherently chiral surfaces or those created by site blocking or surface etching by the chiral modifier that leaves the surface itself chiral.[18−21] When reactants are described as prochiral, achiral gas-phase molecules exhibit surface-bound or point chirality upon adsorption on a surface.

Pioneering work in the McBreen lab has definitively related the molecular scale structure and population of adsorbed 1:1 complexes between reactant and modifier to the enantiomeric excess of an actual reaction.[22] Directly imaging the chiral modifier 2,2,2-trifluoroacetophenone (TFAP) and prochiral molecule 1-(1-naphthyl)ethylamine (NEA), using room-temperature scanning tunneling microscopy (STM), revealed that complexes of many orientations form, for which the chirality of individual components can be determined and analyzed. The observed symmetry breaking in the relative numbers of formed complexes is a direct manifestation of the interaction of (*R*)-NEA with the TFAP chiral modifier on the Pt(111) surface. This work illustrates the powerful approach of using high-resolution STM on model systems in order to understand the molecular origins of symmetry breaking that leads to enantioselectivity.

Discovering and defining these 1:1 interactions and their role in symmetry breaking is necessary for a molecular-level understanding of chiral diastereomeric interactions with chiral modifiers. In this article we present a system of the chiral modifier, propylene oxide (PO), interacting with a similar prochiral molecule, propene (Py), on Cu(111) as a model study for examining the role of 1:1 enantioselective interactions. We chose one of the simplest chiral/prochiral systems and examined it at 5 K in order to use STM-based molecular manipulation to assemble chiral complexes and visualize the chirality of the constituent parts. The small size of the molecules also enabled us to perform density functional theory (DFT)-based calculations to determine the interaction energies and barriers between the adspecies of interest. Related to this, Zaera *et al.* found that the sticking probability of PO molecules is influenced by the chirality of the already adsorbed molecules on Pt(111).[23] Most interestingly, incorporating prochiral propene into this system amplified the enantioselective adsorption of PO on the chirally seeded Pt(111) surface.[24] These results suggest a preference for the conversion of Py, which is achiral in the gas phase, to homochiral arrays of the surface-bound chiral form, but the molecular origin of this effect is not known.

## RESULTS AND DISCUSSION

Before we discuss the enantioselective interactions between PO and Py we must first understand the appearance and dynamics of the individual molecules. Both PO and Py molecules are in fact molecular rotors at 5 K on Cu(111), and the chirality of each can be seen at the single-molecule level. This leads to a simple molecular rotor system in which each molecule has only one structure for each intrinsic or surface-bound chirality, which allows us to visualize and quantify enantioselective interactions.

**Propylene Oxide Molecular Rotors.** The first step in understanding enantioselectivity in this system hinges on our ability to differentiate the chirality of individual adsorbed molecules.[25−27] Internal molecular resolution is difficult to achieve, but imaging of PO on Cu has offered an alternative method of differentiation based on the rotation exhibited by the molecule. At 5 K, molecular diffusion and other dynamic properties are usually inhibited, often resulting in the highest resolution imaging achievable. However, as a molecular rotor at 5 K, PO images as a superposition of six equivalent adsorption geometries, forming a flower-like structure, as seen in Figure 1. Our DFT-based calculations have verified that the

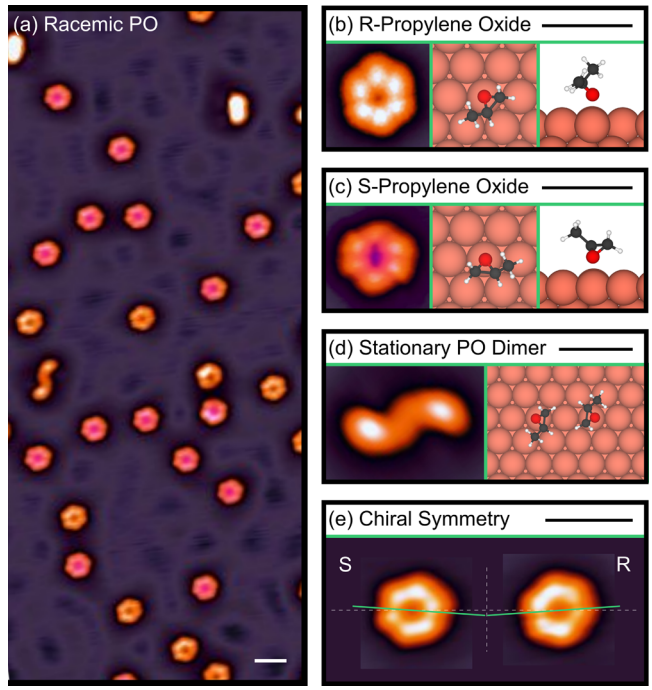


**Figure 1. (a) STM images of a racemic mixture of propylene oxide (PO) on Cu(111) annealed to 40 K. *R*- and *S*-PO molecules are dispersed and rotating on the surface. Scale bars = 1 nm. The *S*-PO molecules are differentiated by a pink highlight. When two PO molecules are close enough together, the interaction between them stops the rotation. For both chiralities, (b) *R*-PO and (c) *S*-PO, rotating PO images are presented as a superposition of six preferred adsorption geometries. One such DFT-computed geometry is depicted. The methyl group, which points away from the Cu(111) surface, appears as a bright protrusion in the STM images. (d) Two *S*-PO molecules form a nonrotating dimer, as illustrated in the DFT-calculated geometry. (e) *S*- and *R*-PO can be differentiated by the fact that their lobes are rotationally offset (green line) from the close-packed direction (horizontal dotted line). The pink, red, gray, and white spheres in the DFT-computed geometries are Cu, O, C, and H atoms, respectively.**

molecule adsorbs atop a Cu atom through the oxygen (epoxide functional group of the molecule), about which rotation occurs; see Figure 1(b,c) and Supporting Information Figure S1. The methyl group is pointed away from the Cu(111) surface and appears as a protrusion in the STM images. Each lobe of the flower-like structure mimics the underlying 6-fold symmetry of the metal substrate, but is offset +4° or −4° from the substrate lattice dependent on the chirality of the adsorbed molecule, Figure 1(e). This method of determining chirality due to rotational symmetries has been found effective in similar circumstances.[28] Upon adsorption through the oxygen there are two possible lone pairs through which PO can adsorb, but experimentally there is only one distinct structure seen for each enantiomer. The intrinsic chirality of the PO molecule is transferred to the surface-bound chiral center at the O atom, as confirmed by DFT.[29] PO on Cu(111) is thus a



DOI: 10.1021/acsnano.9b01781
*ACS Nano* 2019, 13, 5939−5946

simple chiral system with only one adsorption site and geometry for each enantiomer.

PO molecules continuously rotate on the surface unless some steric restraint is applied; rotation occurs at a rate much faster than the time to complete an STM image. Our DFT-based calculations rationalize this observation by verifying that the rotational barrier for PO is very small, on the order of 1 to 5 meV and within the errors of the DFT methods.[30] While lone PO molecules rotate, when in close proximity the PO−PO interaction stops the rotation of both molecules, as seen in Figure 1(d) and Figure S2. This is a reversible process in which STM manipulation can be used to move PO together as well as apart to recover the free rotation, as demonstrated in Figure S3. Most PO molecules are dispersed from one another on the surface, with annealing (80 K) increasing this dispersion, suggesting weak repulsive forces between PO molecules, but these forces are too small to be quantified within the error of our DFT calculations.

**Propene Molecular Rotors.** Propene is achiral in the gas phase, but upon adsorption on Cu(111), it exhibits surface-bound or point chirality (designated *R*′, *S*′). Due to symmetry, equal amounts of each surface-bound enantiomer are to be expected on an achiral surface. Py is also a molecular rotor at 5 K with a calculated rotational barrier of 9 meV, which is within DFT error.[30] It images as a six-lobed structure similar to PO, but has a 3-fold symmetry when considering the brightness of each lobe. There are two propene orientations observed on the surface in equal concentrations corresponding to the two surface-bound enantiomers. The Py molecules clearly repel one another, as they are well separated and no dimers are observed, Figure 2(a). This result is consistent with our DFT calculations, for which a repulsive interaction energy of 0.21 eV is obtained (see Supporting Information Section 3). The 3-fold symmetry of the lobes of rotating propene is the discerning feature between the two enantiomers of the molecule, Figure 2(d).

Our DFT-based calculations indicate that propene adsorbs favorably atop Cu atoms through the C═C $\pi$-bond, with the methyl group angled away from the surface, Figure 2(b) and (c). Atop rotor adsorption is generally 6-fold symmetric, which does not account for the 3-fold symmetry seen in the STM images (see Figure 2(d)), suggesting that all six orientations of propene are not equivalent.[31] However, all starting geometries,[32−36] including those that are 3-fold symmetric, optimized to Py on top of the Cu atom. Our calculations reveal subtle differences between energetic minima during rotation of Py molecules, resulting in some orientations being slightly more stable, hence the rotor residing in these states for longer and hence their lobes being brighter, *e.g.*, states at 0°, 120°, 240° *vs* 60°, 180°, 300°.[30] This explains the 3-fold symmetry and allows us to discern the surface-bound chirality of individual Py molecules (see Supporting Information Section 4). Since Py is less strongly bound to the surface than PO by ∼0.1 eV, it can be manipulated to attractively follow the STM tip at conditions where PO molecules are static. Most translations of Py molecules across the surface, with conditions below 200 mV, 1.7 nA as demonstrated in Figure 2(e) and discussed in the Supporting Information Section 5, do not change the surface-bound chirality of the molecule, with a 3.3% chance of switching orientation when moving a single molecule across the surface. There is only one structure seen for each surface-bound enantiomer of Py, and, as elucidated from our DFT calculations, each structure can be attributed to a specific chirality.

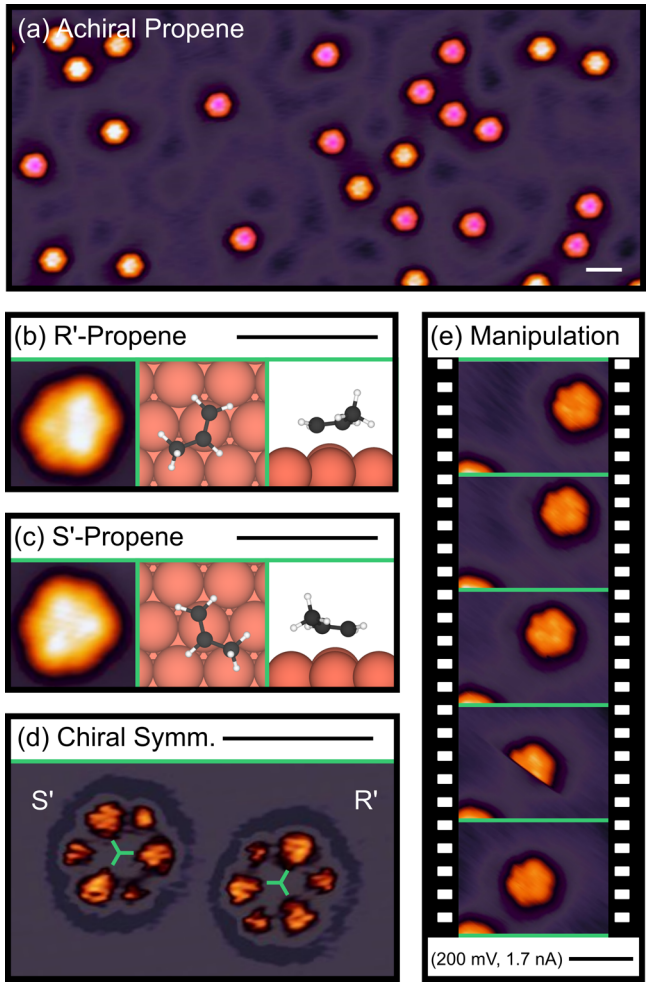


**Figure 2. (a) Propene deposited on Cu(111) and imaged at 5 K. Scale bars = 1 nm. Two rotating configurations are dispersed on the surface in equal concentrations. One configuration is highlighted pink. (b) High-resolution STM image of *R*′-surface-bound propene configuration. DFT-determined lowest energy adsorption geometry. (c) *S*′-surface-bound propene. (d) Filtered version of image emphasizing alternating 3-fold brightness of lobes and electronic perturbation of the surface around the propene molecules. The molecule on the left has an *S*′ surface-bound chirality; the molecule on the right has *R*′ surface-bound chirality. (e) Molecular manipulation of propene; *R*′-surface-bound propene maintains its chirality when translated across the surface with the STM tip. (Horizontal is a close-packed direction in all images; in (e), the scan direction is 45 deg. Tip manipulation conditions are given.) The color coding of the spheres in the DFT-computed geometries is as in Figure 1.**

**Enantioselective Formation of 1:1 Chiral Complexes.** Figure 3 shows results of experiments in which equal amounts of PO and Py were deposited on Cu(111) at 5 K, annealed, and then imaged. Interestingly, while PO and Py do not interact with their own species, co-dosing results in the formation of 1:1 PO:Py complexes. Most significantly, this 1:1 pairing is enantioselective. When *R*-PO and Py are deposited, Figure 3(a) reveals that two types of complexes labeled 1 and 2 are present. Similarly, when *S*-PO and Py are co-deposited, two complexes labeled 3 and 4 are seen, Figure 3(c). Close inspection reveals that the complexes are mirror images of one



DOI: 10.1021/acsnano.9b01781
ACS Nano 2019, 13, 5939−5946

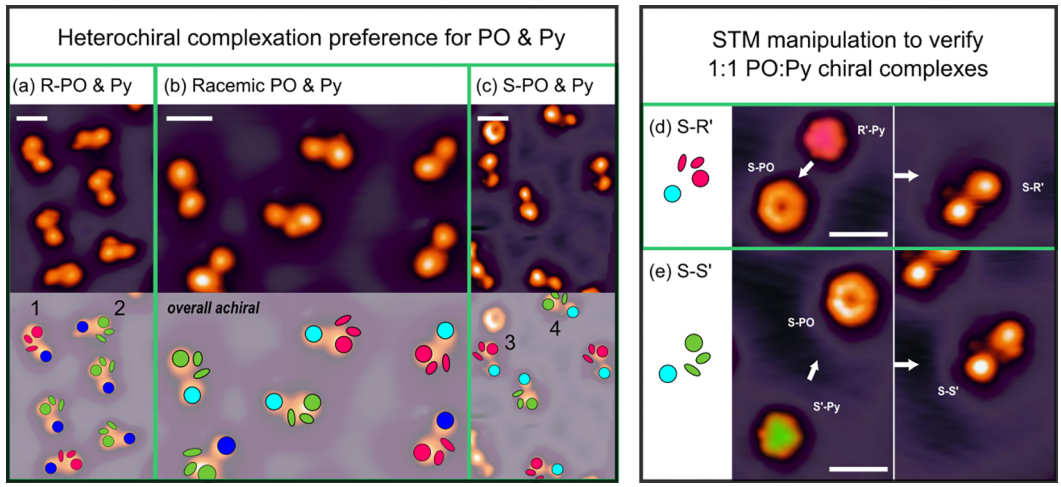


**Figure 3. Interactions between PO and Py on Cu(111) at 5 K form 1:1 chiral complexes enantioselectively, which can be verified with STM manipulation. During spontaneous complexation (a) *R*-PO and Py form two types of chiral complexes (1 and 2), (b) racemic PO (equal *R* and *S* concentration) and Py form four types of chiral complexes (1−4), and (c) *S*-PO with Py forms 1:1 complexes (3 and 4). *R*-PO (dark blue) preferentially complexes with surface-bound *S*-chirality of Py (green). *S*-PO (light blue) favors the surface-bound *R*-chirality of Py (pink). Racemic PO complexation results in the formation of all four complexes. (d) Formation of *S*−*R*′ complex with the STM tip. (e) *S*−*S*′ complexation with the STM tip. The surface-bound orientation of the propene remains after complexation.**

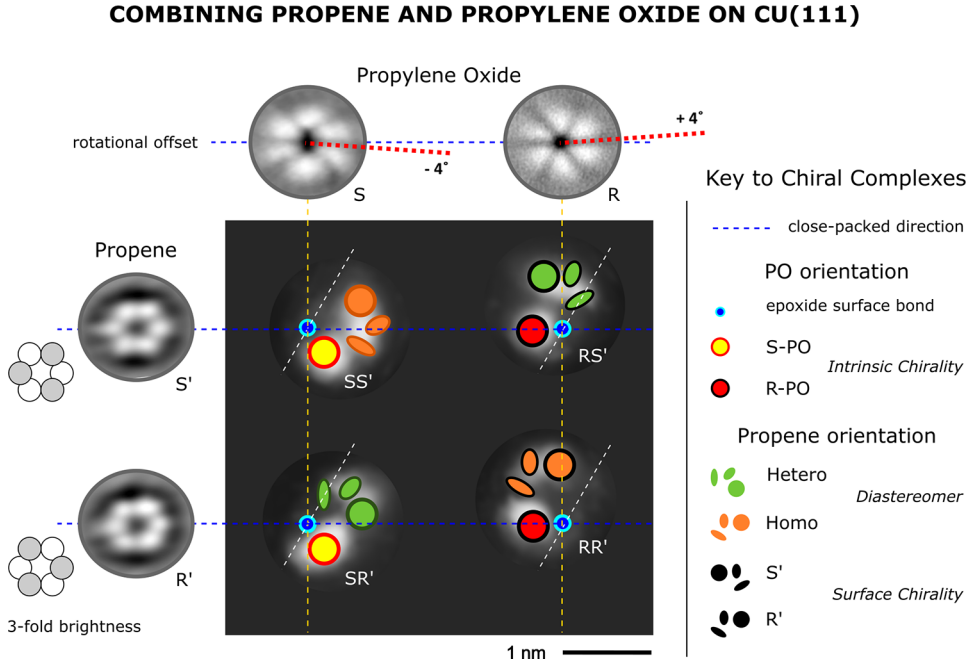


**Figure 4. Visual table of PO and Py 1:1 complex configurations highlighting defining physical features seen in STM images as well as the chirality of each unit of the complex. Rotating propylene oxide (PO) and rotating propene (Py) combine to form four nonrotating complexes (*SR*′, *SS*′, *RS*′, or *RR*′). Notation: *XY*′ is defined as *X* = intrinsic chirality of PO; *Y*′ = surface chirality of Py.**

another (1 and 4) and (2 and 3). Counting over 500 such complexes reveals a preference of orientation 2 over 1 and 3 over 4. Furthermore, when racemic PO is co-dosed with Py, we observe four different 1:1 complexes that are identical to types 1−4 observed in the aforementioned experiments. There is also a preference for types 2, 3 over types 1, 4 in these racemic experiments. Therefore, we are able to observe and quantify the preference for enantioselective binding of one chiral form of adsorbed Py with each PO chirality. To check this preference for enantioselective binding, we first performed molecular manipulation experiments in which we artificially assemble the 1:1 complexes by moving together PO and Py rotors of known chirality. Figure 3(d) and (e) show an overview of these experiments in which the 1:1 PO:Py complex is formed by pulling the Py molecule toward the PO molecule with the STM tip (200 mV, 1.7 pA); for subsequent manipulations including chirality interconversion see Figure S5. Comparison of the appearance of the spontaneously formed complexes in Figure 3(b) and those deconstructed with STM tip manipulations to separate molecules in images of pure PO and Py on the surface (Figures 1 and 2) confirms that the complexes are indeed made from PO:Py pairs. Most significantly the experiments in which the 1:1 complexes are formed with the STM tip provide definitive assignment of the



DOI: 10.1021/acsnano.9b01781
ACS Nano 2019, 13, 5939−5946

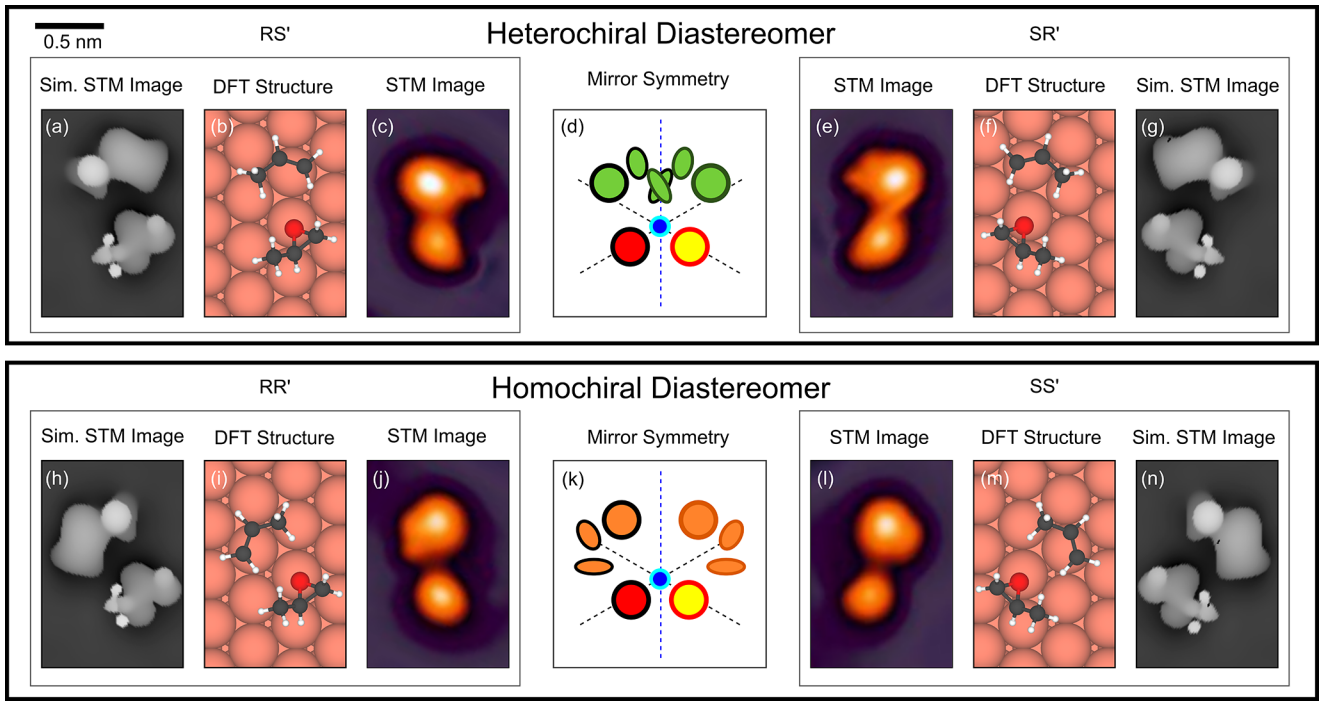


**Figure 5. Intermolecular resolution of 1:1 PO−Py complexes reveals two distinct diastereomers. Here we highlight the symmetry of each diastereomer mirrored across the close-packed direction (vertical). Center panels (d) and (k) schematically represent the symmetry observed, adjacent to which we display the 5 K STM image (0.5 nm scale in top left corner), the DFT-based structure, and the simulated STM image of each complex. Heterochiral diastereomer: (a−c) *RS′* complex: *R*-PO, *S′*-Py (surface-induced). (a) Simulated STM image. (b) DFT-determined structure. (c) STM image. (d) Mirror symmetry of diastereomer. Propene is three green lobes. *S*-PO is red and *R*-PO is yellow. (e−g) *SR′* complex: *S*-PO, *R′*-Py. Homochiral diastereomer: (h−j) *RR′* complex: *R*-PO, *R′*-Py. (k) Mirror symmetry of diastereomer. Propene is three orange lobes. *S*-PO is red and *R*-PO is yellow. (l−n) *SS′* complex: *S*-PO, *S′*-Py. The color coding of the spheres in the DFT-computed geometries is as in Figure 1.**

chirality of the constituent molecules of the four chiral 1:1 complexes.

Combining the two surface-bound propene orientations with the two chiral propylene oxide molecules results in the formation of four distinct chiral complexes. According to our DFT-based calculations (see Supporting Information Section 7), PO:Py complexation is energetically favorable, with an average attractive dimer formation energy of −0.14 eV. Figure 4 summarizes the defining features for PO and Py separately as well as in the 1:1 complex. Complexes can be identified with a two-letter notation based on the intrinsic chirality of PO (*S* or *R*) and the surface-bound chirality of Py (*S′* or *R′*). The four nonrotating complexes are thus labeled *SR′*, *SS′*, *RS′*, and *RR′* and are orientated on the surface as two non-mirror-image diastereomers. The complexes form in six directions commensurate with the underlying high-symmetry directions of the Cu(111) surface. No other 1:1 complex configurations were seen on the Cu(111) surface. Figure 5 illustrates the symmetry of these diastereomers. Each orientation of a diastereomer has an equivalent of opposite chirality mirrored across the close-packed axes; that is, *RS′* is a mirror image of *SR′* and *RR′* is a mirror image of *SS′*. The schematic of this plane of symmetry is shown in Figure 5(d) and (k) with the complex mirrored across the close-packed vertical axis (see key of complex lobes in Figure 4). Taken from the same 5 K STM image, panels (c), (e), (j), and (l) show the mirror-image relationship of the complexes. The DFT-relaxed structure of these complexes ((b), (f), (i), (m)) shows PO and Py sit almost atop on adjacent Cu atoms. Simulated STM images ((a), (g), (h), (n)) reproduce the positions of methyl structural lobes fairly accurately at −0.5 V.

By analyzing all aspects of the PO and Py 1:1 complex system as obtained from STM images, we can utilize this high level of detail and control to define and quantify the enantioselective interactions. Because the submolecular resolution within chiral complexes can directly determine the orientation of the constituent molecules, we combined racemic PO and Py to determine preferences for the formation of particular complexes. Low-coverage racemic PO was deposited on Cu(111) at 5 K and annealed at 40 K to minimize the formation of PO−PO dimers. Py was then deposited at a coverage slightly greater than PO, Figure 3(b). Complexes were formed by annealing to 40 K, allowing the energy necessary for the molecules to interact with molecules of differing surface chirality and orientation before complexation. A discussion of forming exclusively 1:1 PO:Py complexes and other coverages is given in Supporting Information Section 8 and Figure S6. A total of 596 complexes were identified by 5 K STM imaging, and their structures were tabulated to reveal enantioselective pairings, Table 1.

**Table 1. Complexation of PO and Py after a 40 K Anneal**

| complex | population |
|---|---|
| *RS′* | 186 ± 4.3 |
| *SR′* | 174 ± 4.1 |
| *RR′* | 121 ± 3.4 |
| *SS′* | 115 ± 3.4 |



DOI: 10.1021/acsnano.9b01781
*ACS Nano* 2019, 13, 5939−5946

Roughly the same amount of *R*- and *S*-PO are found forming complexes, as a consequence of a racemic mixture. Overall, equal amounts of each surface-bound chirality of Py form complexes, effectively leaving the system with no net chirality. However, more complexes of heterochiral diastereomer orientations are found than homochiral. Table 1 shows for every two homochiral diastereomers, there are approximately three heterochiral. Selectivity in this system arises in that *R*-PO prefers to complex with *S*′-Py, while *S*-PO favors *R*′-Py. As such, heterochiral complexation is more favorable than homochiral (3:2) on Cu(111). In this system as well as others,[22] symmetry breaking was observed to occur regardless of sequence in which the prochiral molecule and the modifier are added to the surface.

Attempts to calculate the relative energies of the four complexes revealed that the energetic differences within this diastereomer system are outside the scope of current DFT calculation accuracy. This was illustrated by the fact that calculations of the energy of the same diastereomer of the opposite chiralities should have the same energy; therefore the difference in this energy is the error of the calculation, effectively benchmarking the accuracy of our DFT results, which we found to be around 14 meV. The differences in the energies of all four complexes are less than this value; thus an energetic preference for one complex over another cannot be calculated by our methods.

## CONCLUSIONS

Propylene oxide is one of the smallest chiral molecules in nature, but experiments have shown that it is an effective chiral modifier that imprints its chirality onto surface-bound propene, which then exhibits enantioselective adsorption properties. This autoamplification is an interesting and somewhat ubiquitous phenomenon in chemistry and biology. By using STM and leveraging its ability to manipulate individual molecules we probe the origin of symmetry breaking in this system. We discover that while propene is achiral in the gas phase, it adsorbs in two enantiomeric forms that can be distinguished by the appearance of the rotating molecules. While propylene oxide and propene do not interact attractively with their own kind, when co-deposited on a surface, we find a predominance of mixed 1:1 pairs. A combination of high-resolution STM imaging, manipulation, and DFT-based calculations allows us to quantify the chirality of each molecule, both in the complexes and in their individual molecular rotor forms. Our results indicate that propylene oxide interacts more favorably with one surface-bound enantiomer of propene, leading to enantiospecific complex formation. As such, despite the very small size of propene, symmetry breaking can occur at the dilute single-molecule limit *via* a 1:1 interaction with the chiral modifier propylene oxide.

## EXPERIMENTAL AND COMPUTATIONAL METHODS

All experiments utilized an Omicron Nanotechnology low-temperature scanning tunneling microscope under ultra-high-vacuum conditions ($10^{-12}$ mbar base pressure). Racemic and enantiopure samples of propylene oxide were acquired from Sigma-Aldrich. The 99% pure liquids were further purified by freeze−pump−thaw cycles, then deposited on a single-crystal Cu(111) surface cleaned by repeated $Ar^+$ sputter and anneal cycles. Propene gas (99.9% pure) was acquired from Matheson Trigas. All molecules were dosed onto the Cu(111) surface held at 5 K. Anneals of 40 or 80 K were utilized to disperse adsorbed molecules or facilitate complexation, after which the temperature was brought back down to 5 K for imaging. Typical conditions for imaging both PO and Py were at a sample bias between ±60 mV and a tunneling current of <70 pA. Scanning conditions increasing sample bias to 200 mV allowed for selective diffusion of Py molecules. STM images in this article have been gain corrected and rotated such that a close-packed direction of the underlying Cu(111) surface is horizontal unless mentioned directly. We have adopted the terminology of McBreen and collaborators[22] for describing 1:1 enantioselective pairings as complexes.

The Cu(111) surface (with a theoretical lattice constant of 3.63 Å) was modeled using a 6 × 6 supercell of four atomic layers to ensure no artificial lateral interactions were present across periodic images. All calculations modeling propylene oxide and propene on this surface were performed with the Vienna *ab Initio* Simulation Package (VASP), which uses the projector augmented wave (PAW) method to project pseudo core electron wave functions onto the atomic centers.[37,38] The PAW pseudopotentials used were from the 2012 release. For modeling of the valence electrons, an energy cutoff of 500 eV was used to determine the plane wave basis set for these electrons. Further, a (2 × 2 × 1) Monkhorst−Pack grid was used to sample the Brillouin zone in these calculations. Structural optimizations performed were considered converged when the total system energy across consecutive electronic steps changed by less than $10^{-6}$ eV and all interatomic forces were less than 0.02 eV/Å. Note that only the top two layers of the Cu(111) supercell and adsorbates were allowed to structurally relax. The exchange−correlation energy was treated using the optB88-vdW functional, which is based on the generalized gradient approximation (GGA) and includes nonlocal corrections to properly capture the adsorption energetics of these molecules on the Cu(111) surface.[39,40] STM images of these optimized structures for comparison with experiment were generated using the Tersoff−Hamann approach with a bias voltage of −0.5 V.[41,42]

## ASSOCIATED CONTENT

### Supporting Information

The Supporting Information is available free of charge on the ACS Publications website at DOI: 10.1021/acsnano.9b01781.

Discussion on DFT-calculated adsorption sites for PO on Cu(111); experiments and discussion on PO STM manipulation; DFT-calculated adsorption sites for Py on Cu(111); 3-fold symmetry of Py; details of experiments involving the translation of Py on Cu(111); additional molecular manipulations with complexes; DFT calculation of interaction energy for complexes; correct ratios of PO:Py to form exclusively 1:1 complexes and errors based on those statistics (PDF)

## AUTHOR INFORMATION


### Corresponding Authors

*E-mail: js.mcewen@wsu.edu.
*E-mail: Charles.Sykes@tufts.edu.

### ORCID

Jean-Sabin McEwen: 0000-0003-0931-4869
E. Charles H. Sykes: 0000-0002-0224-2084


### Notes

The authors declare no competing financial interest.

## ACKNOWLEDGMENTS

The experimental work at Tufts was supported by the National Science Foundation under Grant CHE-1764270. Financial support to WSU was provided by the National Science Foundation CAREER program under contract No. CBET-1653561. A portion of the computer time for the computational work was performed using EMSL, a national scientific



DOI: 10.1021/acsnano.9b01781
*ACS Nano* 2019, 13, 5939−5946

user facility sponsored by the Department of Energy's Office of Biological and Environmental Research and located at PNNL. PNNL is a multiprogram national laboratory operated for the U.S. DOE by Battelle.

## REFERENCES

(1) Blaser, H.-U.; Pugin, B.; Spindler, F. Progress in Enantioselective Catalysis Assessed from an Industrial Point of View. *J. Mol. Catal. A: Chem.* **2005**, *231*, 1−20.
(2) Orito, Y.; Imai, S.; Niwa, S. Asymmetric Hydrogenation of Methyl Pyruvate Using Pt-C Catalyst Modified with Cinchonidine. *Nippon Kagaku Kaishi* **1979**, 1118−1120.
(3) Orito, Y.; Imai, S.; Niwa, S. Asymmetric Hydrogenation of α-Keto Esters Using Platinum-Alumina Catalyst Modified with Cinchona Alkaloid. *Nippon Kagaku Kaishi* **1980**, 670−672.
(4) Izumi, Y. Modified Raney Nickel (MRNi) Catalyst: Heterogeneous Enantio-Differentiating (Asymmetric) Catalyst. *Adv. Catal.* **1983**, *32*, 215−271.
(5) Hoek, A.; Sachtler, W. Enantioselectivity of Nickel Catalysts Modified with Tartaric Acid or Nickel Tartrate Complexes. *J. Catal.* **1979**, *58*, 276−286.
(6) Ortega Lorenzo, M.; Baddeley, C. J.; Muryn, C.; Raval, R. Extended Surface Chirality from Supramolecular Assemblies of Adsorbed Chiral Molecules. *Nature* **2000**, *404*, 376−379.
(7) Yasukawa, T.; Suzuki, A.; Miyamura, H.; Nishino, K.; Kobayashi, S. Chiral Metal Nanoparticle Systems as Heterogeneous Catalysts Beyond Homogeneous Metal Complex Catalysts for Asymmetric Addition of Arylboronic Acids to α,β-Unsaturated Carbonyl Compounds. *J. Am. Chem. Soc.* **2015**, *137*, 6616−6623.
(8) Mahapatra, M.; Burkholder, L.; Garvey, M.; Bai, Y.; Saldin, D. K.; Tysoe, W. T. Enhanced Hydrogenation Activity and Diastereomeric Interactions of Methyl Pyruvate Co-Adsorbed with R-1-(1-Naphthyl)Ethylamine on Pd(111). *Nat. Commun.* **2016**, *7*, 12380.
(9) Wilson, K. E.; Trant, A. G.; Baddeley, C. J. Interaction of the Pro-Chiral Molecule, Methylacetoacetate, with (S)-Aspartic Acid Modified Ni{111}. *J. Phys. Chem. C* **2012**, *116*, 1092−1098.
(10) Parschau, M.; Romer, S.; Ernst, K.-H. Induction of Homochirality in Achiral Enantiomorphous Monolayers. *J. Am. Chem. Soc.* **2004**, *126*, 15398−15399.
(11) Orglmeister, E.; Bürgi, T.; Mallat, T.; Baiker, A. Conformational Rigidity: A Necessary Prerequisite of Chiral Modifiers Used in Heterogeneous Enantioselective Catalysis? *J. Catal.* **2005**, *232*, 137−142.
(12) Kyriakou, G.; Beaumont, S. K.; Lambert, R. M. Aspects of Heterogeneous Enantioselective Catalysis by Metals. *Langmuir* **2011**, *27*, 9687−9695.
(13) Meemken, F.; Hungerbühler, K.; Baiker, A. Monitoring Surface Processes During Heterogeneous Asymmetric Hydrogenation of Ketones on a Chirally Modified Platinum Catalyst by Operando Spectroscopy. *Angew. Chem., Int. Ed.* **2014**, *53*, 8640−8644.
(14) Baiker, A. Crucial Aspects in the Design of Chirally Modified Noble Metal Catalysts for Asymmetric Hydrogenation of Activated Ketones. *Chem. Soc. Rev.* **2015**, *44*, 7449−7464.
(15) Meemken, F.; Baiker, A.; Schenker, S.; Hungerbühler, K. Chiral Modification of Platinum by Co-Adsorbed Cinchonidine and Trifluoroacetic Acid: Origin of Enhanced Stereocontrol in the Hydrogenation of Trifluoroacetophenone. *Chem. - Eur. J.* **2014**, *20*, 1298−1309.
(16) Rodíguez-García, L.; Hungerbühler, K.; Baiker, A.; Meemken, F. Discrimination of Active Species in Liquid-Phase Hydrogenation on Supported Noble Metal Catalyst: An Operando Spectroscopic Study on the Asymmetric Hydrogenation of Ketopantolactone on Pt/$Al_2O_3$ and Pt/C Modified by Cinchonidine. *Catal. Today* **2017**, *283*, 66−73.
(17) Goubert, G.; Dong, Y.; Groves, M. N.; Lemay, J.-C.; Hammer, B.; McBreen, P. H. Monitoring Interconversion Between Stereochemical States in Single Chirality-Transfer Complexes on a Platinum Surface. *Nat. Chem.* **2017**, *9*, 531−536.
(18) Gellman, A. J.; Tysoe, W. T.; Zaera, F. Surface Chemistry for Enantioselective Catalysis. *Catal. Lett.* **2015**, *145*, 220−232.
(19) Yun, Y.; Gellman, A. J. Adsorption-Induced Auto-Amplification of Enantiomeric Excess on an Achiral Surface. *Nat. Chem.* **2015**, *7*, 520−525.
(20) Durán Pachón, L.; Yosef, I.; Markus, T. Z.; Naaman, R.; Avnir, D.; Rothenberg, G. Chiral Imprinting of Palladium with Cinchona Alkaloids. *Nat. Chem.* **2009**, *1*, 160−164.
(21) Jenkins, S. J.; Pratt, S. J. Beyond the Surface Atlas: A Roadmap and Gazetteer for Surface Symmetry and Structure. *Surf. Sci. Rep.* **2007**, *62*, 373−429.
(22) Demers-Carpentier, V.; Goubert, G.; Masini, F.; Lafleur-Lambert, R.; Dong, Y.; Lavoie, S.; Mahieu, G.; Boukouvalas, J.; Gao, H.; Rasmussen, A. M. H.; Ferrighi, L.; Pan, Y.; Hammer, B.; McBreen, P. H. Direct Observation of Molecular Preorganization for Chirality Transfer on a Catalyst Surface. *Science* **2011**, *334*, 776−780.
(23) Karakalos, S.; Lawton, T. J.; Lucci, F. R.; Sykes, E. C. H.; Zaera, F. Enantiospecific Kinetics in Surface Adsorption: Propylene Oxide on Pt(111) Surfaces. *J. Phys. Chem. C* **2013**, *117*, 18588−18594.
(24) Karakalos, S.; Zaera, F. Amplification of Enantioselectivity on Solid Surfaces Using Nonchiral Adsorbates. *J. Phys. Chem. C* **2015**, *119*, 13785−13790.
(25) Lopinski, G. P.; Moffatt, D. J.; Wayner, D. D. M.; Wolkow, R. A. Determination of the Absolute Chirality of Individual Adsorbed Molecules Using the Scanning Tunnelling Microscope. *Nature* **1998**, *392*, 909−911.
(26) Ernst, K.-H.; Baumann, S.; Lutz, C. P.; Seibel, J.; Zoppi, L.; Heinrich, A. J. Pasteur's Experiment Performed at the Nanoscale: Manual Separation of Chiral Molecules, One by One. *Nano Lett.* **2015**, *15*, 5388−5392.
(27) Ernst, K.-H. Stereochemical Recognition of Helicenes on Metal Surfaces. *Acc. Chem. Res.* **2016**, *49*, 1182−1190.
(28) Tierney, H. L.; Murphy, C. J.; Jewell, A. D.; Baber, A. E.; Iski, E. V.; Khodaverdian, H. Y.; McGuire, A. F.; Klebanov, N.; Sykes, E. C. H. Experimental Demonstration of a Single-Molecule Electric Motor. *Nat. Nanotechnol.* **2011**, *6*, 625−629.
(29) Liriano, M. L.; Carrasco, J.; Lewis, E. A.; Murphy, C. J.; Lawton, T. J.; Marcinkowski, M. D.; Therrien, A. J.; Michaelides, A.; Sykes, E. C. H. The Interplay of Covalency, Hydrogen Bonding, and Dispersion Leads to a Long Range Chiral Network: The Example of 2-Butanol. *J. Chem. Phys.* **2016**, *144*, No. 094703.
(30) Groden, K.; Larson, A. M.; Hannagan, R. T.; Sykes, E. C. H.; McEwen, J.-S. Elucidating the Nature of Molecular Rotations on Single-Crystal Surfaces. To be submitted for publication.
(31) Tierney, H. L.; Jewell, A. D.; Baber, A. E.; Iski, E. V.; Sykes, E. C. H. Dynamics of Molecular Adsorption and Rotation on Nonequilibrium Sites. *Langmuir* **2010**, *26*, 15350−15355.
(32) Nykänen, L.; Honkala, K. Density Functional Theory Study on Propane and Propene Adsorption on Pt(111) and PtSn Alloy Surfaces. *J. Phys. Chem. C* **2011**, *115*, 9578−9586.
(33) Valcácel, A.; Ricart, J. M.; Clotet, A.; Markovits, A.; Minot, C.; Illas, F. Theoretical Study of the Structure of Propene Adsorbed on Pt(111). *Surf. Sci.* **2002**, *519*, 250−258.
(34) Toomes, R. L.; Lindsay, R.; Baumgärtel, P.; Terborg, R.; Hoeft, J.-T.; Koebbel, A.; Schaff, O.; Polcik, M.; Robinson, J.; Woodruff, D. P.; Bradshaw, A. M.; Lambert, R. M. Structure Determination of Propyne and 3,3,3-Trifluoropropyne on Cu(111). *J. Chem. Phys.* **2000**, *112*, 7591−7599.
(35) Valcárcel, A.; Ricart, J. M.; Clotet, A.; Markovits, A.; Minot, C.; Illas, F. Structure and Bonding of Propyne on Cu(111) from Density Functional Periodic and Cluster Models. *J. Chem. Phys.* **2002**, *116*, 1165−1170.
(36) Parschau, M.; Passerone, D.; Rieder, K.-H.; Hug, H.; Ernst, K.-H. Switching the Chirality of Single Adsorbate Complexes. *Angew. Chem., Int. Ed.* **2009**, *48*, 4065−4068.
(37) Kresse, G.; Furthmüller, J. Efficient Iterative Schemes for Ab Initio Total-Energy Calculations Using a Plane-Wave Basis Set. *Phys. Rev. B: Condens. Matter Mater. Phys.* **1996**, *54*, 11169−11186.



DOI: 10.1021/acsnano.9b01781
*ACS Nano* 2019, 13, 5939−5946

(38) Kresse, G.; Hafner, J. Ab Initio Molecular Dynamics for Liquid Metals. *Phys. Rev. B: Condens. Matter Mater. Phys.* **1993**, *47*, 558−561.
(39) Klimeš, J.; Bowler, D. R.; Michaelides, A. Chemical Accuracy for the van der Waals Density Functional. *J. Phys.: Condens. Matter* **2010**, *22*, No. 022201.
(40) Klimeš, J.; Bowler, D. R.; Michaelides, A. Van der Waals Density Functionals Applied to Solids. *Phys. Rev. B: Condens. Matter Mater. Phys.* **2011**, *83*, 195131.
(41) Tersoff, J.; Hamann, D. R. Theory and Application for the Scanning Tunneling Microscope. *Phys. Rev. Lett.* **1983**, *50*, 1998−2001.
(42) Tersoff, J.; Hamann, D. R. Theory of the Scanning Tunneling Microscope. *Phys. Rev. B: Condens. Matter Mater. Phys.* **1985**, *31*, 805−813.



DOI: 10.1021/acsnano.9b01781
*ACS Nano* 2019, 13, 5939−5946